chemistry proceedings

MDPI

Proceedings

First principles investigation of the optoelectronic properties of Molybdenum dinitride for optical sensing applications †

A.A. Ramanathan

The University of Jordan, Department of Physics, Amman-11942, Jordan
Correspondence: amallahmad@gmail.com

† Presented at CSAC2021: 1st International Electronic Conference on Chemical Sensors and Analytical Chemistry, online, 01-15/07/2021.

Abstract: The electronic and optical properties of the newly synthesized Molybdenum dinitride (MoN_2) in the hypothetical 2H structure analogous to MoS_2 is investigated using the Density Functional Theory (DFT) full potential linearized augmented plane wave (FP-LAPW) method and the Modified Becke-Johnson (mBJ) approximation. The aim is to investigate the optoelectronic properties of this compound for potential optical sensing applications and compare with the capabilities of MoS_2 in this field. As compared to MoS_2, which is a semiconductor, MoN_2 is found to be a semi metal from the band structure plots. The dielectric function, optical conductivity and the optical constants, namely, the refractive index, the reflectivity, the extinction and absorption coefficients are evaluated and compared with those of MoS_2 and discussed with reference to the sensing performance.

Keywords: Layered materials; Electronic structure; Dielectric function; Optical conductivity; optical constants; optical sensing

1. Introduction

The high potential of transition metal dichalcogenides (TMD) for electronic, sensing, photonic and thermoelectric device applications has been exploited this past decade and especially MoS_2 a prototype TMD material has shown a lot of promise [1-3]. It has been studied and characterized extensively for structural, electronic, optical and transport properties both in bulk and in the 2D limit [4-6]. Interest in TM nitrides has been rekindled because they exhibit a number of unique and advanced catalytic properties for photo and electrochemical catalysis [7, 8]. There were no layered structures in any of these studies. Layered structures provide more flexibility in doping, ease of going down to lower dimensions and materials design.

The search for layered nitrogen rich TM nitrides, particularly those of MoS_2-type, led to the recent synthesis and discovery of 3R–MoN_2, which has the rhombohedral MoS_2 structure [9]. It was synthesized through a high P–T route of solid-state ion-exchange and has shown great potential for applications in catalysis and hydrogenation. In addition, the very recent first principles study of MoN_2 monolayer by Zhang et al [10] showed the 1H configuration to be the most stable among the structures considered in their study. Their study revealed the importance of 2D MoN_2 as a high capacity electrode material for metal ion batteries. Further, the first principles study of Ramanathan and Khalifeh [11] has shown the 2H MoN_2 to be a promising thermoelectric material.

All the above interesting results for MoN_2 provide a strong motivation to study this compound. Considering that, to date no optical characterization of MoN_2 has been performed; the present study is devoted to the determination of the electronic and optical properties from first principles and to look at the various possibilities for optical sensing

Published: 1 July 2021

applications of MoN_2. Since, an optical sensor measures a physical property of light and depending upon the sensor usage converts it to a readable output, it is highly essential to characterize the optical properties of the new layered material MoN_2. The hypothetical 2H structure analogous to MoS_2 of MoN_2 is investigated using the DFT full potential linearized augmented plane wave (FP-LAPW) method and the mBJ approximation. In addition, the 2H MoS2 optoelectronic properties are determined by the same method for the sake of completeness and comparison.

2. Calculation details

The geometry of MoN_2 is optimized using the ABINIT software program [12, 13] with the generalized gradient approximation (GGA) of Perdew, Burke and Ernzerhof (PBE) PAW (projector augmented wave) pseudopotentials [14]. All the structural calculations are performed with convergence criteria of less than 1×10^{-6} Ha for the Self Consistent Field (SCF) iterations and a threshold of less than 1 mRy/a.u. for the optimization of the geometries [15, 16]. The fully relaxed MoS_2 lattice constant values are taken from our previous work [6].

The optimized structures and lattice constant values are then used with the WIEN2k [17] code to perform full-potential linearized-augmented plane wave (FP-LAPW) calculation employing GGA_PBE to obtain the ground state energy and electronic properties at a 20×20×4 k-point grid. The optical properties are evaluated using denser grids of 40×40×5 with the more accurate mBJ exchange correlation of Trans Blaha (TB-mBJ).

3. Results and discussion

3.1. Structural and electronic

The 2H-MoN2/MoS2 unit cells have hexagonal symmetry and consist of two stacks of 3 atomic layers; each stack consists of a Mo atomic plane sandwiched between two N/S atomic planes respectively. The atoms are bonded covalently in plane and the stacks are held together by weak Van der Waals force.

The non-magnetic state is the ground state for both the layered compounds and the structural relaxation of the system with a complete relaxation of all the atoms simultaneously gives us the equilibrium geometry. The lattice parameter a and c values of MoN_2 are 3.094 and 11.975Å respectively. The lattice parameter values of MoN_2 are much smaller than that of MoS_2 due to the shorter bond lengths of Mo-N as compared to Mo-S. The lattice parameters for MoS_2 a=3.193 and c=12.359Å taken from previous work [6] using the LDA (local density approximation) are in good agreement with the experimental values [19] a_{exp}=3.16Å and c_{exp} = 12.29Å and within 2.3 and 0.6% respectively.

The equilibrium lattice constant values for MoN_2 and MoS_2 are used with the GGA-PBE Wien2k code to extract the electronic band structures with a 20×20×4 k-point grid

We notice that there is a change in the electronic distribution of MoN_2 as compared to MoS_2 which is reflected in the band structure of MoN_2 as shown in Figure1. The MoS_2 band structure is also shown on the right panel of Figure1. The band structures illustrate the change in behavior of MoN_2 to a semi metal one from the semiconducting one of MoS_2. There is an overlap between the bottom of the conduction band and the top of the valence band in MoN_2. This semi metal feature implies that there is a range of energies for which electrons and holes co-exist. The Mo 4d, S 3p and N 2p atomic orbitals play a decisive role in the band structure properties.

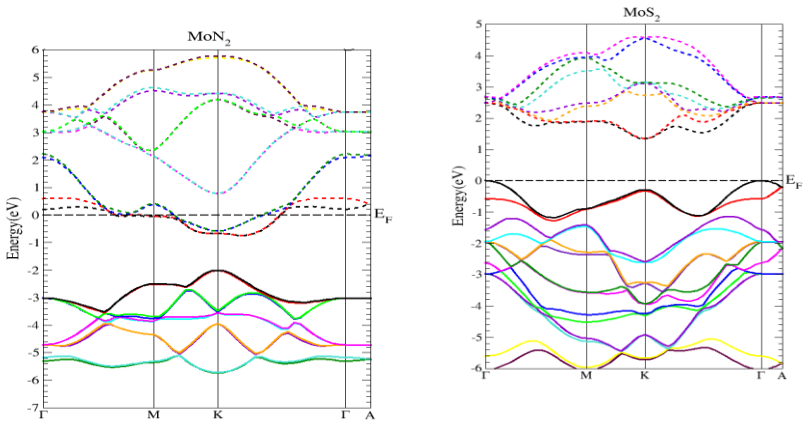

(**a**) (**b**)

Figure 1. The band structures of (a) MoN_2 and (b) MoS_2.

3.2. Optical Properties

The TB-mBJ proves to be an excellent choice with a 40×40×5 grid for calculating the optical properties with a high degree of accuracy for MoN_2 and MoS_2. This section is devoted to the presentation and discussion of the results for the dielectric function and optical conductivity. In addition, the optical constants namely the refractive index, the reflectivity, the extinction and absorption coefficients are obtained and interpreted.

The complex dielectric function ($\varepsilon = \varepsilon_1 + i\varepsilon_2$) is a function of the amount of light absorbed by the material. The imaginary part of dielectric function, $\varepsilon_2(\omega)$, which represents absorption behavior, can be calculated from the electronic band structure of solids. The real part of dielectric function, $\varepsilon_1(\omega)$, which represents the electronic polarization under incident light can be calculated according to Kramers-Kroing relation [20, 21]. Figure 2 shows the real and imaginary plots for the dielectric function for MoN_2 and MoS_2 in the photon energy range of 0-14eV. We see from the plots the anisotropy of the dielectric function. The general trend is the in-plane values are almost double that of the out of plane direction and the peaks are shifted more towards the right with higher energies.

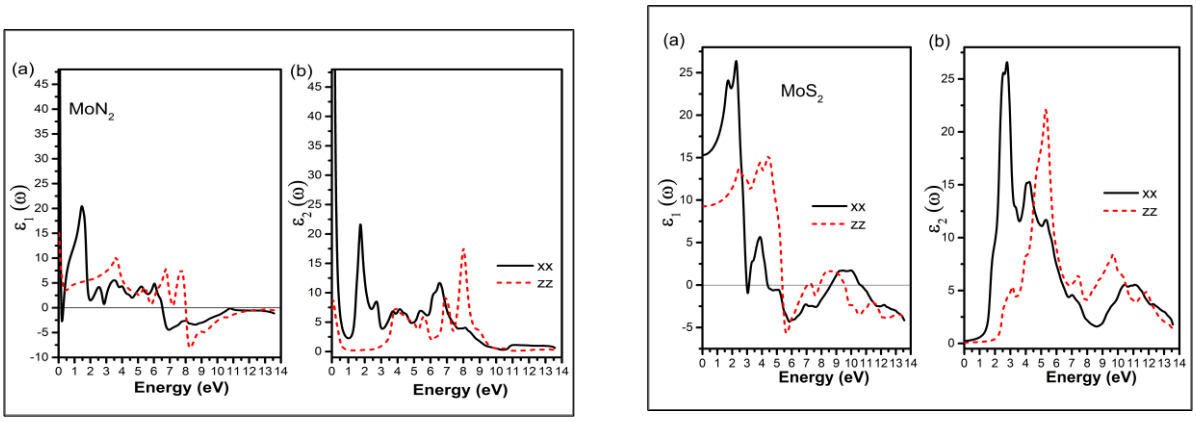

Figure 2. The dielectric function left panel MoN_2 right panel MoS_2; (a) the real $\varepsilon_1(\omega)$ and (b) imaginary part $\varepsilon_2(\omega)$ for the in-plane (xx) and out of plane (zz) directions.

The complex index of refraction of the medium N is defined as $N = \sqrt{\varepsilon} = n + ik$

Where n is the refractive index and k the extinction coefficient. These are depicted in Figure 3.

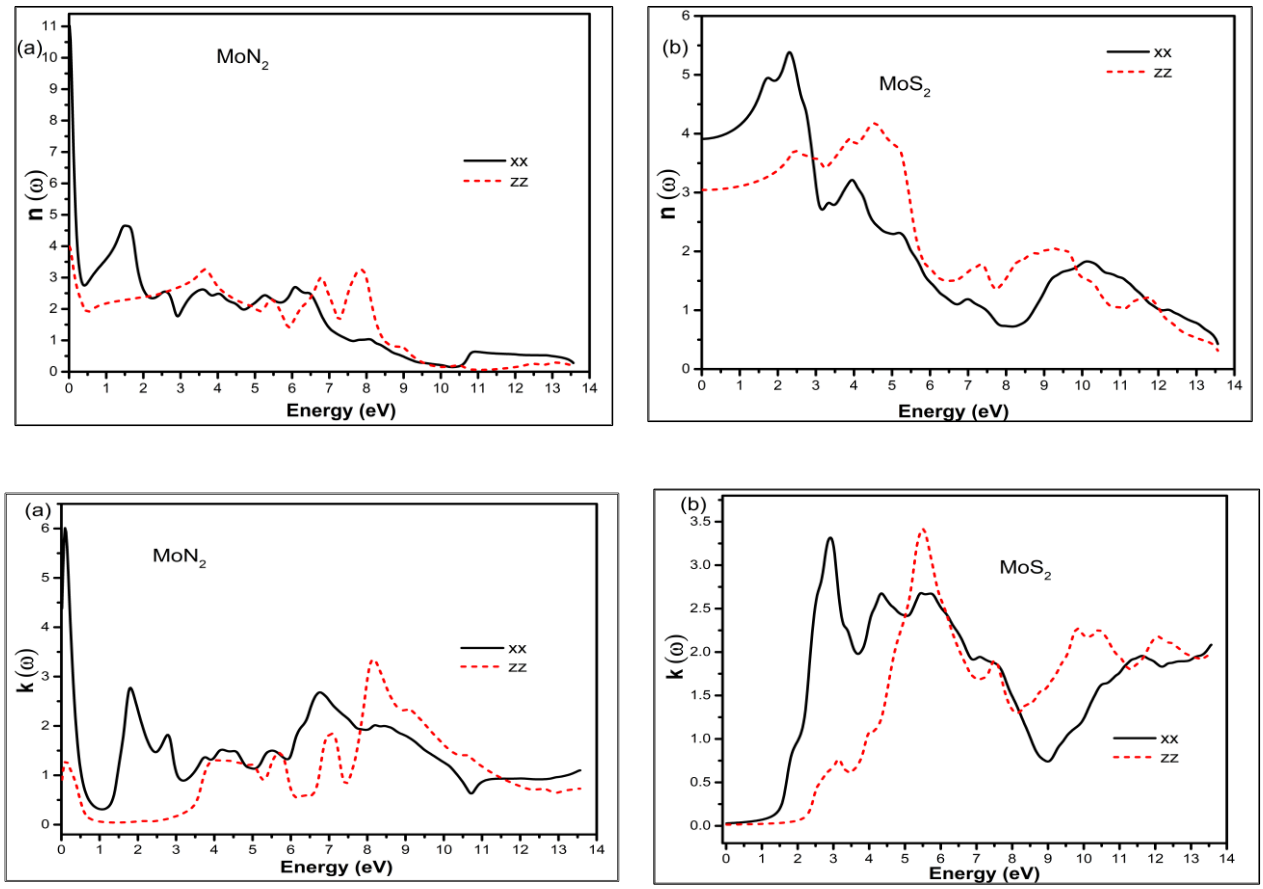

Figure 3. The refractive index top panel and extinction coefficient bottom panel for MoN_2 and MoS_2 in the xx in-plane and zz out of plane directions.

Once again we see the anisotropy in the two directions for these optical constants. The amplitudes in the xx direction is larger and closer to the visible range for both n (ω) and k (ω) for both compounds. We notice that MoN_2 has large static (ω=0) refractive index values of ~11 and 4 in the xx and zz directions respectively. In contrast the corresponding values for MoS_2 are 4 and 3. The larger values of n(ω) imply higher electron density. In contrast to MoS_2, MoN_2 has peak extinction coefficient values at ω =0 of 4.4 and 0.9 in the xx and zz directions respectively. Both MoN_2 and MoS_2 show low k(ω) values in the infra red and MoS_2 continues to have almost zero values upto 1.5 and 2.5eV for xx and zz directions respectively. The first maxims of MoS_2 are at 3eVof the spectra and the magnitude in the xx direction almost six times larger than in the zz direction. The second k peak for zz direction is in the UV region and slightly larger than the first xx peak.

The conductivity and absorption coefficient graphs for MoN_2 and MoS_2 are shown in Figure 4.

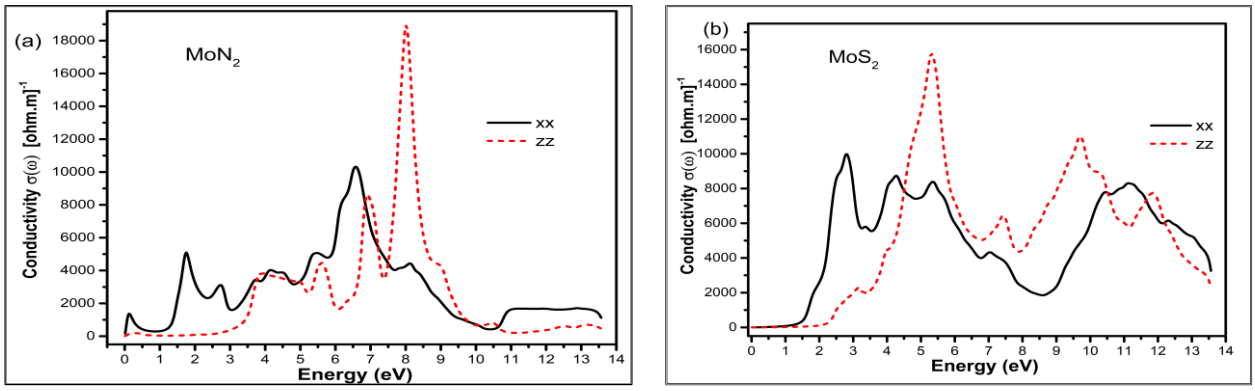

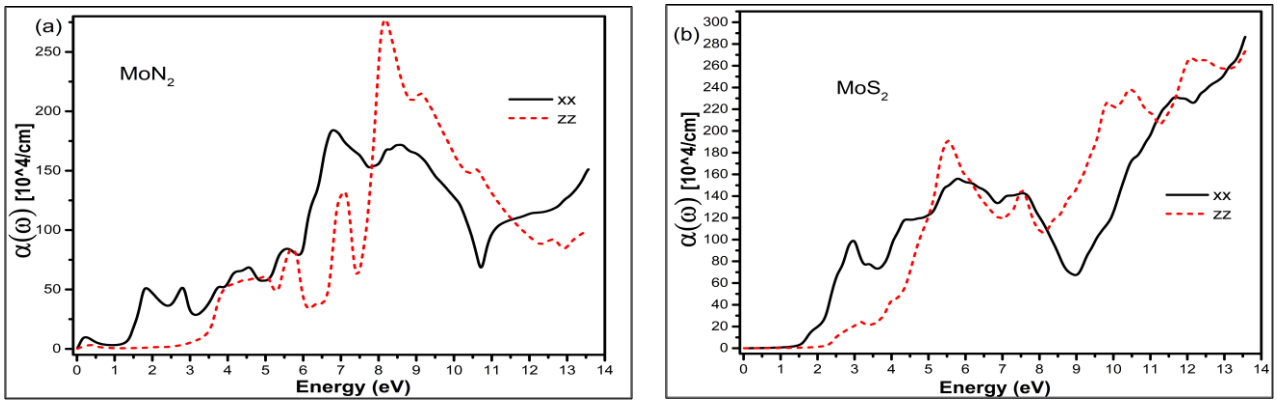

Figure 4. The optical conductivity top panel and absorption coefficient bottom panel for MoN_2 and MoS_2 in the xx in-plane and zz out of plane directions.

The graphs show for the xx in-plane direction maximum conductivity is in the UV region for MoN_2 whereas for MoS2 it is in the visible part of the photon energy. The conductivity in the zz direction has peak positions in the UV region around 8 and 5eV for MoN_2 and MoS_2 respectively. The absorption on the other hand shows the first peak in the visible and second broader peak with a much higher magnitude in the UV region for MoN_2; and a very broad peak of almost constant magnitude for MoS_2 covering the visible and the UV region in the in plane xx direction. Beyond 10eV both MoN_2 and MoS_2 show a rise in the absorption coefficient. With respect to the zz direction there are a set of small peaks beyond the visible and a sharp maximum value peak at around 9eV of the UV region for MoN_2; whereas for MoS_2 the peaks are around 6, 10 and 12eV in the UV region. These characteristics confirm the suitability of MoN_2 and MoS_2 for visible and UV sensing applications. The reflectance is depicted in Figure 5 and we observe large static reflectance value greater than 0.7 for MoN_2 that is double of MoS_2 in the xx direction. In the zz direction the values are 0.35 and 0.25 for MoN_2 and MoS_2 respectively. The graphs show that MoN_2 is a good infra-red reflector, whereas MoS_2 reflects best just beyond the visible range.

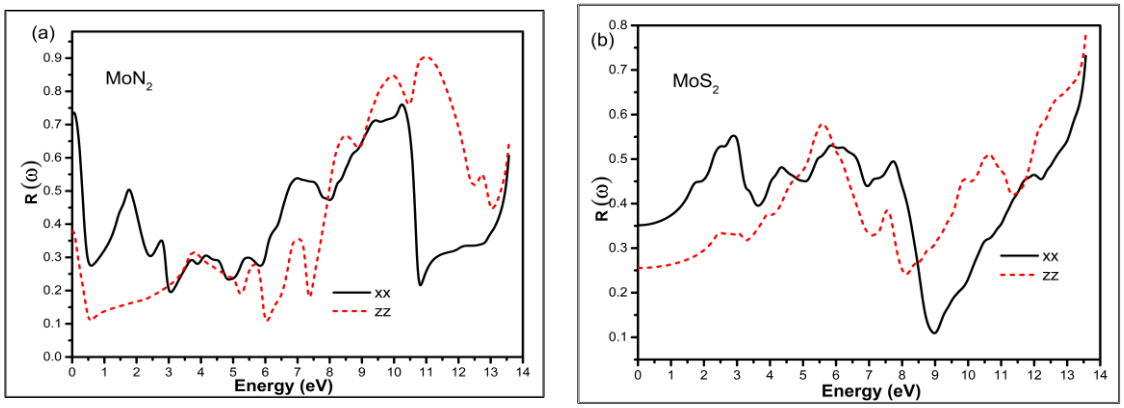

4. Conclusions

In conclusion as opposed to MoS_2, MoN_2 is a semi metal. Both layered materials show anisotropy for all the optical properties with different magnitudes and peak positions, although the shapes of the graphs for the same property are similar in the two directions.

The large values of refractive index and good conductivity, absorption and reflectance results obtained reinstate the suitability of these materials for sensing applications in the visible and UV region.

References

1. N. Onofrio, D. M. Guzman, A. Strachan. Novel doping alternatives for transition metal dichalcogenides from high-throughput DFT calculations. *Journal of Applied Physics* **122**, 185102 (2017).
2. Y. H. Wang, K.J. Huang and X. Wu: Recent advances in transition-metal dichalcogenides based electrochemical biosensors: A review. *Biosens Bioelectron,* **97**, 305 (2017). doi: 10.1016/j.bios.2017.06.011.
3. D. Vikraman, K. Akbar, S. Hussain, G. Yoo, J-Y. Jang, S-H. Chun, J. Jung, H.J. Park: Direct synthesis of thickness-tunable MoS_2 quantum dot thin layers: Optical, structural and electrical properties and their application to hydrogen evolution. *Nano Energy*, **35**, 101 (2017).
4. A.A. Ramanathan: Defect Functionalization of MoS_2 nanostructures as toxic gas sensors. *IOP Conf. Ser.: Mater. Sci. Eng.* **305** 012001 (2018). doi:10.1088/1757-899X/305/1/012001
5. H. Zhang, S. B. Lu, J. Zheng, J. Du, S. C. Wen, D. Y. Tang, and K. P. Loh, "Molybdenum disulfide (MoS_2) as a broadband saturable absorber for ultra-fast photonics," Opt. Express 22, 7249-7260 (2014)
6. A.A. Ramanathan and J.M. Khalifeh: Enhanced thermoelectric properties of suspended mono and bilayer of MoS2 from first principles. *IEEE Transactions on nanotechnology*, **17(5),** 974, (2018).
7. Chen, W.-F.; Muckerman, J. T.; Fujita, E. Chem. Commun. 2013, 49, 8896.
8. Tabata, M.; Maeda, K.; Higashi, M.; Lu, D.; Takata, T.; Abe, R.; Domen, K. Langmuir 2010, 26, 9161.
9. S. M. Wang, H. Ge, S. L. Sun, J. Z. Zhang, F. M. Liu, X. D. Wen, X. H. Yu, L. P. Wang, Y. Zhang, H. W. Xu, J. C. Neuefeind, Z. F. Qin, C. F. Chen, C. Q. Jin, Y. W. Li, D.W. He and Y. S. Zhao. A New Molybdenum Nitride Catalyst with Rhombohedral MoS_2 Structure for Hydrogenation Applications. *J. Am. Chem. Soc.*, **137**, 4815 (2015).
10. X. Zhang, Y. Yao, Z. Yu, S-S Wang, S. Guan, H. Y. Yang, and S. A. Yang (2016). Theoretical prediction of MoN2 monolayer as a high capacity electrode material for metal ion batteries. J. Mater. Chem. A, 4, 15224
11. Ramanathan A A and Khalfeh JM Thermoelectrics of MoS2(1-x)N2x Compounds. *Phys Sci & Biophys J* **2021**, *5 (1)*, 000167. DOI: 10.23880/psbj-16000167
12. A. A. Ramanathan. A DFT calculation of Nb and Ta (001) Surface Properties, *JMP_ Special issue-DFT* **2013**, *4*, 432-437.
13. X. Gonze, F. Jollet, F. A. Araujoa, D. Adams, B. Amadon, T. Applencourt et al (2016). Recent developments in the ABINIT software package. *Computer Physics Communications* 205, 106
14. J. P. Perdew, K. Burke, and M. Ernzerhof, Generalized Gradient Approximation Made Simple, Phys. Rev. Lett. (1996) 77, 3865
15. A.A. Ramanathan and J.M Khalifeh (2017). Substrate matters: Magnetic tuning of the Fe monolayer. *JMMM* 426, 450-453.
16. A. A. Ramanathan, J.M. Khalifeh, and B.A. Hamad (2008). Evidence of surface magnetism in the V/Nb(0 0 1) system: A total energy pseudopotential calculation. *Surf. Sci.* 602, 607
17. P. Blaha, K.Schwarz, F. Tran, R. Laskowski, G.K.H. Madsen and L.D. Marks, J. Chem. Phys. (2020) 152, 074101
18. F. Tran, P. Blaha, Accurate band gaps of semiconductors and insulators with a semilocal exchange-correlation potential, Phys. Rev. Lett. 102 (2009) 226401.
19. R. Coehoorn, C. Haas, J. Dijkstra, C. J. F. Flipse, R. A. de Groot, and A. Wold (1987). Electronic structure of MoSe2, MoS2, and WSe2. I. Band-structure calculations and photoelectron spectroscopy. *Phys. Rev. B* 35 6195
20. Rolf Hulthén. Kramers–Kronig relations generalized: on dispersion relations for finite frequency intervals. A spectrum-restoring filter. *J. Opt. Soc. Am.* **1982,** 72, 794-803
21. Ramanathan A.A.; Khalifeh J.M. Electronic, magnetic and optical properties of XScO3 (X=Mo, W) perovskites *PeerJ Materials Science* 3:e15 https://doi.org/10.7717/peerj-matsci.15